The effect of processing temperature and time on the structure and fracture characteristics of self-reinforced composite poly(methyl methacrylate)

D. D. WRIGHT, J. L. GILBERT*
Department of Biomedical Engineering, Northwestern University, Technological Institute, 2145 Sheridan Road, Evanston, IL 60208, USA

E. P. LAUTENSCHLAGER
**Division of Biological Materials, Northwestern University, 311 E. Chicago Ave., Chicago, IL 60611, USA*

A novel material, self-reinforced composite poly(methyl methacrylate) (SRC-PMMA) has been previously developed in this laboratory. It consists of high-strength PMMA fibers embedded in a matrix of PMMA derived from the fibers. As a composite material, uniaxial SRC-PMMA has been shown to have greatly improved flexural, tensile, fracture toughness and fatigue properties when compared to unreinforced PMMA. Previous work examined one empirically defined processing condition. This work systematically examines the effect of processing time and temperature on the thermal properties, fracture toughness and fracture morphology of SRC-PMMA produced by a hot compaction method. Differential scanning calorimetry (DSC) shows that composites containing high amounts of retained molecular orientation exhibit both endothermic and exothermic peaks which depend on processing times and temperatures. An exothermic release of energy just above T_g is related to the release of retained molecular orientation in the composites. This release of energy decreases linearly with increasing processing temperature or time for the range investigated. Fracture toughness results show a maximum fracture toughness of 3.18 MPa $m^{1/2}$ for samples processed for 65 min at 128 °C. Optimal structure and fracture toughness are obtained in composites which have maximum interfiber bonding and minimal loss of molecular orientation. Composite fracture mechanisms are highly dependent on processing. Low processing times and temperatures result in more interfiber/matrix fracture, while higher processing times and temperatures result in higher ductility and more transfiber fracture. Excessive processing times result in brittle failure.

1. Introduction

Poly(methyl methacrylate) (PMMA) is well known as a glassy, brittle polymer. One of its many uses is as a cementing material in total hip replacements. Polymerizing PMMA is inserted into the femoral canal, a hip prosthesis is positioned in the PMMA, and as the PMMA polymerizes, it solidifies to anchor the implant in place. The low fracture toughness, and poor fatigue properties of PMMA at body temperature, however, have been implicated in failures of these implants [1–3]. For this application, and for others requiring PMMA, improvements in the toughness and fatigue properties would be advantageous. To date, however, only modest improvements in mechanical properties have been achieved in PMMA, usually with the addition of short reinforcing fibers such as carbon [4, 5] or Kevlar [6]. In addition to only providing modest improvements in mechanical properties, these additional components in a biological system may lead to biocompatibility problems [5].

In this laboratory, we have developed a method to melt-spin PMMA into high strength fibers [7]. These fibers can subsequently be processed into high strength self-reinforced composites (SRC) using a sintering, or hot compaction method [8, 9]. The outer surface polymer of the fibers interdiffuses to bond with adjacent fibers, which forms the matrix of the composite directly from the fibers. The resultant composite has both a reinforcing phase and matrix phase consisting of PMMA, thus introducing no new components to the human body.

Other investigators have also used hot compaction methods to fabricate composites. Work has been done with polymers including polyglycolide [10] and polylactide [11] resorbable structures for bone fixation,

*To whom correspondence should be addressed at the Division of Biological Materials. E-mail: eplauten@nwu.edu.

polypropylene [12], polyethylene terephthalate [13] and polyethylene [14–18]. Investigation of processing–structure–property relationships remains a topic of study in these materials. All of this work also deals with semicrystalline polymers, and has not dealt with non-resorbable biomaterial applications. SRC-PMMA is unique in that it is fabricated from amorphous PMMA with significant amounts of molecular orientation.

Our previous work investigated the mechanical properties of uniaxial SRC-PMMA [8], and three different weaves of SRC-PMMA [9]. The second study also investigated the effects of saline immersion and gamma irradiation on the mechanical properties of woven SRC-PMMA. Both studies, however, utilized an empirical method to determine and examine one processing condition. The goal of this study is to vary the processing conditions (primarily time and temperature) and examine the effects of these variations on the thermal behavior, fracture toughness and fracture morphology of SRC-PMMA.

2. Materials

2.1. Fiber fabrication

Fibers were spun (Hills, Inc., W. Melbourne, FL) according to the heat deformation process described previously [7] using PMMA pellets (Atohaas, V045, Philadelphia, PA) at a melt temperature of 260 °C. The molecular weight of the PMMA pellets was determined by four column gel permeation chromatography standardized with polystyrene (Arro Laboratory, Joliet, IL). The number average molecular weight of this acrylic is 26 000 g mol^{-1}, and the weight average of the acrylic is 210 000 g mol^{-1} resulting in a polydispersity of 8.3. The fiber tows contained multiple filaments, with a maximum of 144 in each tow. Minimal fiber breakage during processing caused the number of fibers per tow to vary slightly. Each fiber was approximately 39 μm in diameter. The tensile strength of each fiber was approximately 200 MPa.

2.2. Sample fabrication

Uniaxial composite samples were created by wrapping fiber tows 150 times around a guide. This guide ensured the unidirectional nature of the composite. Fibres were placed in an aluminum channel mold, and a press bar secured with three c-clamps provided pressure. The guide was then removed. The pressure used to incorporate the samples is unknown. During processing, the fibers are constrained which limits the oriented polymer chains from relaxing. Processing of the samples took place in an oven at three different temperatures: 128, 140 and 151 °C. Samples at 128 °C were processed at a range of times, from 30 to 175 min. The samples processed at 140 and 151 °C were processed for 35 min. After processing in the oven, the samples were removed, and the c-clamps, which had loosened, were tightened. During processing, the matrix of the composite is formed from the outer surface of the fibers. As the fibers are heated above the glass transition, the outer polymer chains interdiffuse into neighboring chains to bond the fibers together and form the matrix. However, the constraint of the channel mold slowed the relaxation. The samples were allowed to air cool at room temperature for 10 min before removal from the mold. After processing, the samples ranged from partially to fully transparent, and depending on processing, highly birefringent. Their nominal size was 120 × 13 × 3 mm.

Each bar was used in its entirety to complete the differential scanning calorimetry (DSC) and fracture toughness tests. This ensured that the DSC results could be correlated directly to the fracture toughness results, and not be affected by variations between samples.

2.3. Differential scanning calorimetry samples

Samples weighing between 4.7 and 11.4 mg (8.55 ± 1.75 mg) were sectioned from the SRC-PMMA bars using a diamond wafer blade with an Isomet 11-1180 low speed saw (Beuler, Lake Bluff, IL). The DSC samples were each contained in an aluminum pan with an aluminum lid. SRC-PMMA samples exhibit birefringence under polarized light, appearing bright and colorful. It was observed that near the edges of the bar, the colors were different than in the middle portions of the bar. Therefore, to eliminate edge effects, DSC and fracture toughness samples were sectioned from the portions of the bar, as shown in Fig. 1.

2.4. Fracture toughness samples

Single-edge notched fracture toughness samples were sectioned from the SRC-PMMA bar, as shown in Fig. 1. After sectioning, a crack was placed in the composite material. The crack was begun with the Isomet saw, and a sharp razor blade was lightly tapped in the crack to make it sharper. The crack was placed so that it would propagate toward the center of the original bar before sectioning in order to eliminate any edge effects on the mechanical performance of the composite. The size of the finished samples was 41.30 ± 1.22 mm in overall length, 2.47 ± 0.20 mm in thickness (b) and 6.33 ± 0.26 mm in width (W). The crack size, a, was between the values of $0.45W \leq a \leq 0.55W$, as in the ASTM standard [19].

Control samples were fabricated from acrylic pellets, the raw material for the fiber production. The acrylic pellets were melted in an oven at 200 °C in a crucible for

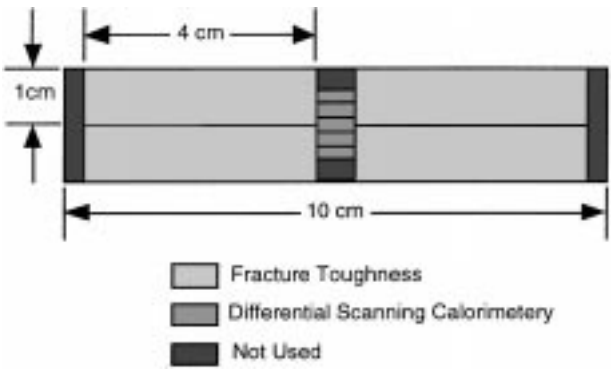

Figure 1 Schematic of DSC and fracture toughness sample sectioning with nominal dimensions shown. Samples are nominally 3 mm thick.

approximately 1 h, and then pressed into a sheet. Once the polymer had solidified, a band saw was used to section the acrylic, and the final shape was attained by polishing the sample with the Handimet grinder with 600 grit sandpaper. The nominal dimensions were the same as those for the composite samples.

3. Methods

3.1. Differential scanning calorimetry

A Perkin Elmer DSC-2 and a computer with an A/D board were used to collect the data. Through preliminary experimentation with amorphous PMMA, a heating rate of 80 °C min^{-1} with a range of 0.5mcals^{-1} was chosen. The choice of this heating rate and its effects will be addressed in the discussion. The sample was heated from 40 to 270 °C. This temperature range was chosen because it is well above and below the typically reported glass transition temperature of 105 °C [20]. The upper limit on the temperature range is just above the temperature at which PMMA begins to decompose, at about 262 °C [21]. Samples were weighed before and after testing until it became evident that no measurable polymer degradation was occurring.

The computer collected the resultant voltage signal with a program developed in this laboratory. The program averages three consecutive voltage values to reduce the noise in the signal, and records the instrument settings. The board samples voltage values at 10 Hz with a gain of 100.

Data collection began slightly before each run to collect an isothermal baseline voltage. Each sample was tested two to four consecutive times. If the second run appeared to be representative of amorphous acrylic, it was determined that additional runs were unnecessary as they would simply overlap the second scan. The isothermal baseline that was collected before the data collection began was designated as the line of zero power. As such, the average power value of this line was subtracted from all the power values in that run. The voltage values that were collected were converted to power values using the A/D board parameters and the DSC instrument parameters. Exothermic and endothermic peak magnitudes and temperatures were recorded for each sample tested.

3.2. Fracture toughness

The samples were tested on the Instron Model 1114 (Cambridge, MA). The crosshead speed was 2.54 mm/min., and the support span (L) was set to a nominal value of 28.0mm. Most of the SRC-PMMA groups had four samples tested; two of the SRC-PMMA bars had only two samples tested. The control group had five samples.

The load at failure (P) was measured using the offset slope method [19,22]. A line was constructed using the initial linear portion of the load-deflection curve. The slope was calculated, and a second line was drawn which represented a 5% reduction of the slope. The load at failure was taken as the point where this second line intersected the load-deflection curve. If the load-deflection curve was linear up to the maximum load, as for sheet acrylic, the maximum load was used for P. Using the sample geometry and P, the fracture toughness was calculated according to [22],

$$K_{IC} = \frac{3PL}{2bW^{3/2}}\left[1.93\left(\frac{a}{W}\right)^{1/2} - 3.07\left(\frac{a}{W}\right)^{3/2} + 14.53\left(\frac{a}{W}\right)^{5/2} - 25.11\left(\frac{a}{W}\right)^{7/2} + 25.80\left(\frac{a}{W}\right)^{9/2}\right]$$

where K_{IC} is the plain strain fracture toughness for mode I fracture (MPa $\cdot$ m$^{1/2}$), P is the offset or maximum load (N), L is the support span (mm), b is the sample thickness (mm), W is the sample height (mm) and a is the crack length (mm).

3.3 Statistical analysis

Statistical analysis of fracture toughness data was performed using a one-way analysis of variance and a post-hoc Neuman Keuls test. A $p \leq 0.05$ was considered significant. The independent variable was considered to be the unique combination of the time and temperature processing variables. The dependent variable was the fracture toughness.

DSC data was quantitatively analyzed using regression analysis. The independent variable was the processing time or temperature and the dependent variable was the exothermic peak height. Regression lines were fit to the data and evaluated based on goodness of fit and whether the line was an accurate predictor of the relationship.

3.4 Scanning electron microscopy

Representative fracture toughness samples were selected to examine with scanning electron microscopy (SEM). Samples at each temperature and a selection of times were examined to determine what differences processing led to in the fracture mechanisms. All samples were mounted in acrylic, and coated with gold to facilitate imaging, except where noted. An SEM (Model S10, Cambridge Instruments, Deerfield, IL) was used to image all surfaces.

4. Results

Samples were viewed under polarized light to determine if there was retained molecular orientation in the composites. When SRC-PMMA samples have retained molecular orientation in the fibers, the composites appear bright and colorful under polarized light. Samples processed at 128 °C for a range of times show the full spectrum of possible colors, ranging from pale reds to bright blues, yellows to grey (with increasing time). This indicates that a wide range of the retained molecular orientation possible for this processing method is being considered. It should be stated that there was a loss in birefringent color when processing times were greater than 65 min at 128 °C. Samples processed at high times (90 and 175 min) have very little birefringence, indicating that there is an upper limit on the processing time before significant loss of retained molecular orientation. Colors for the samples processed for 35 min at a range of temperatures also show the full range of birefringent colors.

4.1. Differential scanning calorimetry

Differential scanning calorimetry results are shown as a function of processing time (Fig. 2) and as a function of processing temperature (Fig. 3). The first scan of the material represents the oriented polymer, and the energies involved in the various relaxation processes that occur. The second and remaining scans of the material represent the behavior of the amorphous, relaxed polymer. It should be noted that due to the alignment of the isothermal baseline prior to testing, all scans subsequent to the first scan (second to the fourth) are superimposed on one another. This allowed determination of relative exothermic and endothermic excursions of oriented composite compared to the relaxed polymer. Note that both the exothermic and endothermic excursions of the oriented polymer compared to the relaxed polymer. These excursions appeared to be sensitive to both processing time (at constant temperature, Fig. 2), as well as temperature (at constant time, Fig. 3). Also shown in these figures is the T_g (ca. 120 °C) which is higher than usually reported for PMMA due to the high scan rate.

In Fig. 4, a running average plot has been constructed from the location and magnitude of all of the peaks in the DSC plots. The magnitude of the peaks were calculated by subtracting the relaxed polymer scan from the oriented polymer scan and measuring the location (temperature) and height (power/mass of sample) of the resulting peaks. A listing was then made of the location and magnitude of all DSC peaks, and was sorted from lowest to highest temperature. From these listings, running averages were calculated independently for both the location (temperature) and magnitude (power/mass of sample) of the peaks. A running average averages a group of points (in this case, 20), and using this method, clusters of points can be more easily identified. As seen in Fig. 4, there are five distinct clusters of peaks. These peaks encompass the endothermic temperature ranges of 110–130 °C, 185–200 °C and 215–235 °C with original peak values from 0–0.1 cal s^{-1} g^{-1}. The exothermic temperature ranges are from 130–135 °C, and a broader cluster from 145–160 °C with original peak magnitudes from -0.1–0 cal s^{-1} g^{-1}.

Figs 5 and 6 were constructed using only the peaks located in the temperature range of 125 to 175 °C that were not related to the glass transition temperature. Peaks in this temperature range represent the energy being released as the polymer molecules lose their retained molecular orientation. Fig. 5 shows the results of plotting exothermic peak height versus processing time for a constant temperature. Fig. 6 shows the data for the samples processed for a common time at different temperatures. If all of the peak heights in Fig. 5 are considered, there is no statistical trend. However, all polymer relaxation has occurred when SRC-PMMA is processed for longer than 70 min, as seen by a loss in birefringence above that time. Regression analysis shows a linear correlation between peak height and processing time (Fig. 5) when peak heights from processing times

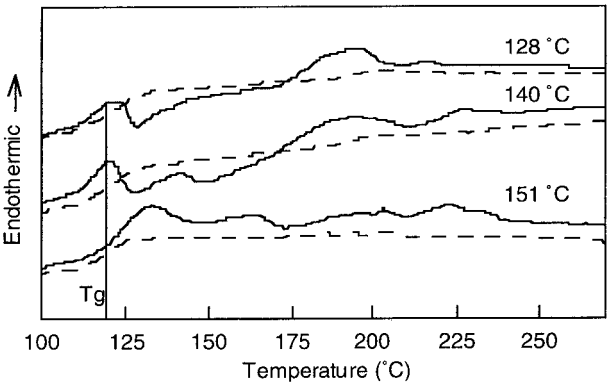

Figure 3 DSC results for samples processed for 35 min at 128, 140 and 151 °C. The solid line represents the first scan of the material, or the oriented SRC-PMMA. The dotted line represents the second scan of the material, or amorphous PMMA. A scan rate of 80 °C min^{-1} was used.

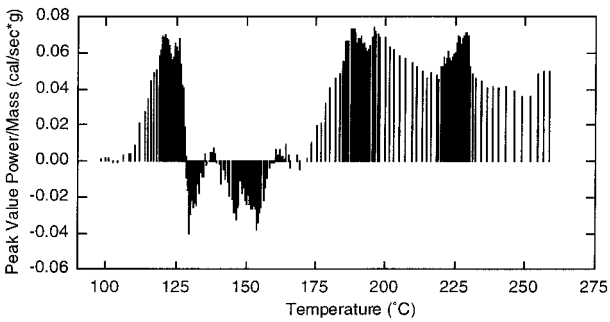

Figure 4 Running average plot of peak height values versus temperature for all DSC peak values. Running average averages groups of 20 points

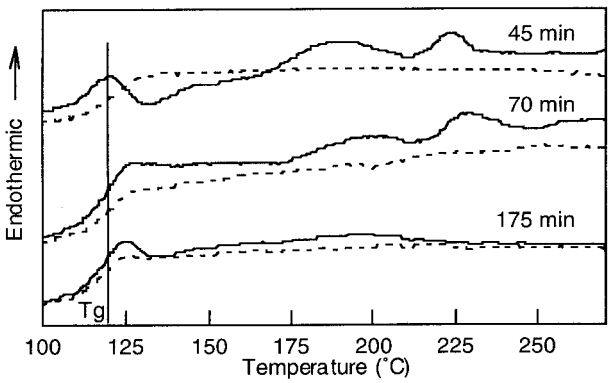

Figure 2 DSC results for samples processed at 128 °C for times ranging from 45 min to 175 min. The solid line represents the first scan of the material, or the oriented SRC-PMMA. The dotted line represents the second scan of the material, or amorphous PMMA. A scan rate of 80 °C min^{-1} was used.

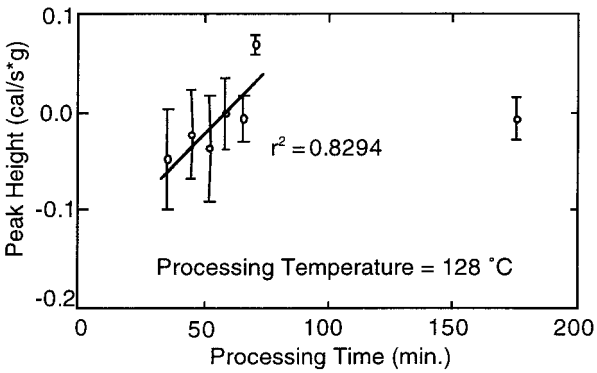

Figure 5 Plot of exothermic peak height versus processing time for samples processed at 128 °C. A linear correlation is seen for the data ($r^2 = 0.8924, P \leq 0.05$) when samples which have lost all of their molecular orientation are not included in the regression analysis (175 min sample).

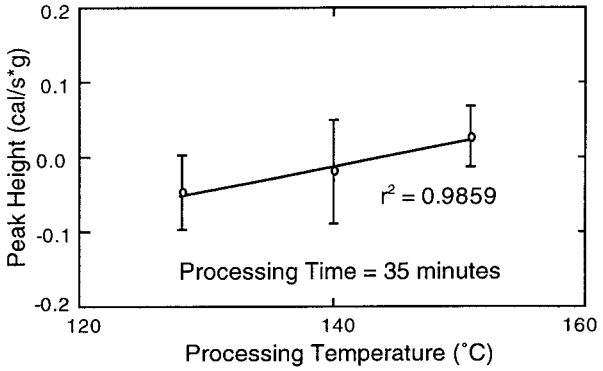

Figure 6 Plot of exothermic peak height versus processing temperature for samples processed for 35 min. A linear correlation is seen for the data ($r^2 = 0.9859, P \leq 0.05$).

greater than 70 min are not included ($P \leq 0.05$). Regression analysis also shows a positive correlation for the relationship between exothermic peak height versus processing temperature (Fig. 6, $P \leq 0.05$).

4.2. Fracture toughness

Fig. 7 shows the fracture toughness results for samples which were processed at a common temperature of 128 °C with a range of times. Error bars are shown for all points, and are representative of plus and minus one standard deviation. A simple line connects points. Fig. 8. has results from samples which were processed for 35 min at 128, 140 and 151 °C. Table I contains the results of the statistical analysis. Comparisons which resulted in a $P \leq 0.05$ are considered significant. Although $P \leq 0.05$ was considered significant, all of the positive comparisons in Table I actually fulfill the criteria $P \leq 0.005$.

4.3. Fracture morphology

Examination of the fracture toughness samples shows some interesting crack morphologies. It was first noted optically that the crack propagation proceeded in different directions for different processing parameters, as shown in Fig. 9. At 128 °C, samples processed at low times (between 35 and 45 min, top sample, Fig. 9) have cracks which propagate perpendicular to the pre-crack. At longer processing times (approximately 50–65 min, middle sample, Fig. 9) or intermediate temperatures (140 °C) the crack proceeds at an angle away from the pre-crack. Composites that have crack propagation perpendicular or at an angle to the pre-crack do not break, but extensive fiber deformation is noted optically along the crack propagation path. When samples are processed at long times (greater than 65 min, bottom sample, Fig. 9) or high temperatures (151 °C), the crack propagates along the same direction as the pre-crack, in a manner similar to the brittle failure of bulk acrylic. There is some overlap in these phenomena, as samples processed for 65 min exhibit crack propagation at an angle to the crack tip and parallel to the crack tip for different samples. As detailed in Table I, it can be seen that samples with different crack propagation directions also have different fracture toughness values, with the angled crack paths yielding the highest fracture toughness.

SEM analysis of the fracture surfaces shows five distinct fracture mechanisms. One fracture mechanism involves the transverse fracture of fibers. When the fracture surface of these fibers can be viewed, lines which indicate the direction of the crack propagation can be seen. A second mechanism is fiber tearing or splitting along the fiber axis, and a third mechanism is cracking along the matrix (i.e. interfiber fracture). These three mechanisms are pictured in Fig. 10. This figure is a detail from a sample processed for 40 min at 128 °C. The pre-crack is oriented vertically and perpendicular to the plane of the micrograph in the center, and the crack has propagated in a direction 90° from the pre-crack to each side of the shown picture. This surface has been cut from the composite to expose the fracture surface. Fibrils are noted (see lower right), indicating splitting of the fibers, and on the upper left, a transverse fiber fracture can be seen. Finally, pieces of matrix material can be seen as tags on some of the fibers (lower left, Fig. 10), and the fiber surfaces are exposed, indicating matrix cracking. Also note that the fibers have assumed a polygonal cross-section as a result of the heat and pressure deformation during processing.

A fourth fracture mechanism is exhibited by the flat, fast fracture of bulk unreinforced PMMA, as shown in Fig. 11. The fracture radiates out from the crack tip in the plane of the pre-crack, and then proceeds in a fast

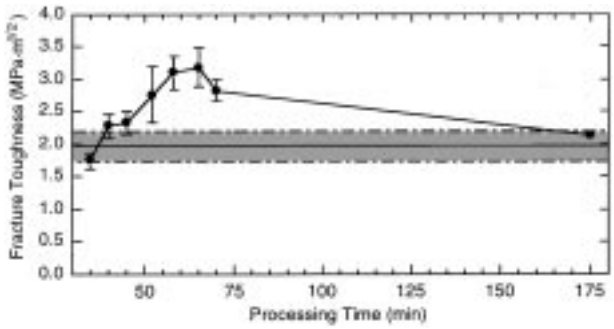

Figure 7 Fracture toughness of uniaxial SRC-PMMA plotted versus time. All samples were processed at a temperature of 128 °C. The horizontal line and gray box represents the mean and standard deviation, respectively, of the acrylic material from which the fibers were fabricated.

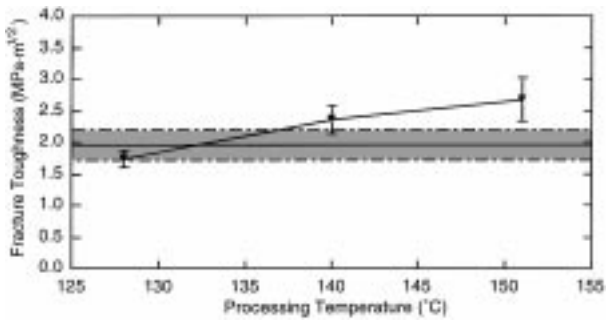

Figure 8 Fracture toughness of uniaxial SRC-PMMA plotted versus temperature. All samples were processed at a time of 35 min. The horizontal line and gray box represents the mean and standard deviation, respectively, of the acrylic material from which the fibers were fabricated.

TABLE I *Post-hoc* statistical results from fracture toughness data shown in Figs 7 and 8

Time			35	35	35	40	45	52	58	65	70	175
	Temp	V045	128	140	151	128	128	128	128	128	128	128
	V045				+			+	+	+	+	
35	128				+			+	+	+	+	
35	140								+	+		
35	151	+	+									
40	128								+	+		
45	128								+	+		
52	128	+	+									
58	128	+	+	+		+	+					+
65	128	+	+	+		+	+					+
70	128	+	+									
175	128								+	+		

Shaded areas represent comparisons between samples processed at a common temperature or time.
+ indicates a significant difference at $P \leq 0.05$.

fracture, as evidenced by the smooth surface. A fifth mechanism is similar to the fast fracture in that the crack radiates out from the pre-crack in a flat manner, however the surface has ripples, indicating a more ductile fracture, as shown in Fig. 14.

Examination of the crack tip of a sample processed for 40 min at 128 °C shows that the crack tip propagates directly perpendicular from the pre-crack along the fiber direction into the matrix. No fiber cleavage is noted at the crack tip. Examination of the fracture surface as shown in Fig. 10 shows fiber cleavage does occur in the bulk composite, however, as well as fiber splitting. It appears that the crack predominantly propagates along the matrix, until conditions are favorable for fiber cleavage or splitting. By far, however, the dominant mechanism of failure in this sample is fracture along the fiber interface.

The crack tip of a sample processed for 58 min at 128 °C is pictured in Fig. 12. As can be seen, fiber cleavage and matrix cracking both play a role in the initial crack propagation at the crack tip. In this sample, the crack initially stayed in the fracture plane, but then turned and continued at an angle into the material. Closer examination of the exposed fracture surface in Fig. 13

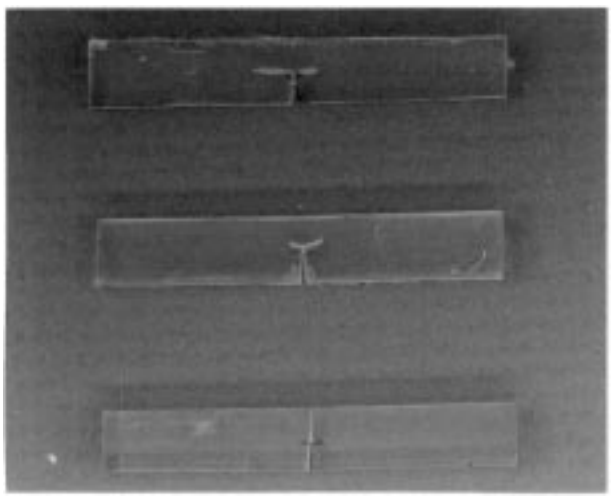

Figure 9 Uniaxial SRC-PMMA fracture propagation. From top to bottom, the samples were processed at the following conditions: 40 min, 128 °C; 58 min, 128 °C; and 70 min, 128 °C. Note the direction of the crack propagation as it varies from the top to bottom sample.

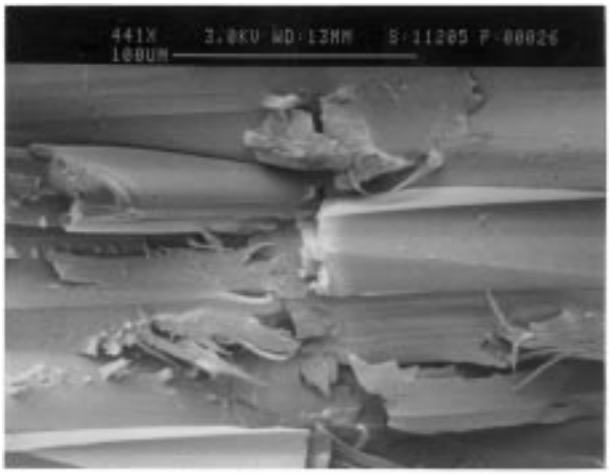

Figure 10 Fracture surface of uniaxial SRC-PMMA processed for 40 min at 128 °C. Fracture toughness is $2.27 \pm 0.19\,\mathrm{MPa\,m^{1/2}}$. The crack is propagating from the center of the picture to both sides. Fibre cleavage, fiber splitting and matrix cracking can be seen.

shows that there is a mixed mode of continued crack propagation. The crack proceeds in a step-like fashion, with a combination of matrix cracking and fiber cleavage (or shearing at an angle to the fiber direction). Contrast the appearance of fibers in this figure with Fig. 10, a sample processed at a shorter time. The composite processed at a longer time is just beginning to lose the distinct appearance of fibers, with increasing fiber–fiber bonding. There is still enough retained molecular orientation in this sample to provide increased toughness.

When processed at longer times (greater than 65 min) or at temperatures greater than 151 °C, the fracture surface is flat, but never approaches the glassy appearance of bulk PMMA for the times and temperatures examined in this study. A typical fracture surface for these high time or high temperature samples is shown in Fig. 14. This micrograph depicts a sample processed for 70 min at 128 °C. Note that the surface is rippled for the entire width of the propagated crack. This indicates that even though the distinct fibers have been lost, there is still some strengthening from the fibers and processing method. In some of these samples, small depressions are noted, which are on the same order of dimensions of

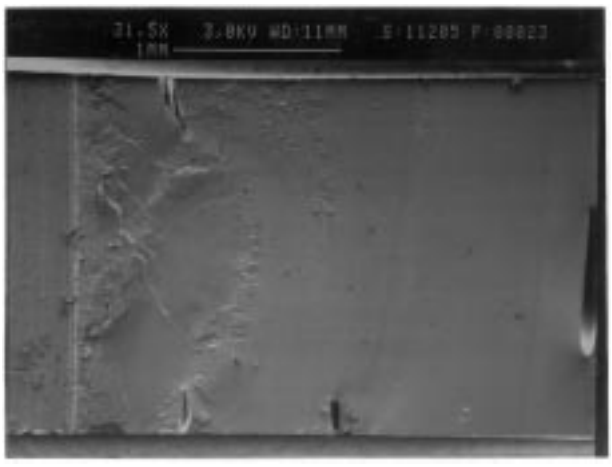

Figure 11 Fracture of bulk PMMA. Fracture toughness is $1.96 \pm 0.24\,\mathrm{MPa\,m^{1/2}}$. Crack propagates from the left to right.

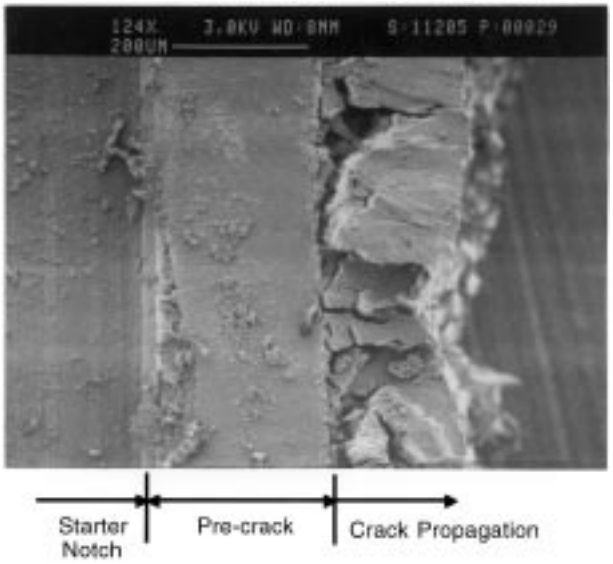

Figure 12 Crack propagation at the crack tip of a sample processed for 58 min at 128 °C. Fracture toughness is 3.10 ± 0.26 MPa m$^{1/2}$. The starter notch is seen at the far left of the micrograph, with the pre-crack formed by the razor blade immediately adjacent. Crack propagation then proceeds from left to right. Note the propagation of the crack continues perpendicular to the pre-crack after about 200 µm. Matrix cracking and fiber cleavage can be seen.

fibers, indicating that some random fibers or molecular orientation may be retained on a small scale.

Uniaxial SRC-PMMA processed for 35 min at 140 °C showed a mixed mode failure very similar to the sample processed for 58 min at 128 °C which is shown in Fig. 12. The crack tip of this sample processed at an intermediate temperature is similar to that shown in Fig. 12, and the fracture surface is shown in Fig. 15. Note that the fracture surface in Fig. 15 shows more distinct fibers than the sample processed for 58 min at 128 °C (Fig. 13), with some evidence of interfiber matrix polymer.

SEM analysis shows distinctive fracture mechanisms occur for different processing methods. For samples processed at low times and temperatures, matrix cracking (i.e. interfiber fracture) is the predominant mechanism, indicating that fiber sintering has not fully occurred. At moderate times and low temperatures, or low times and

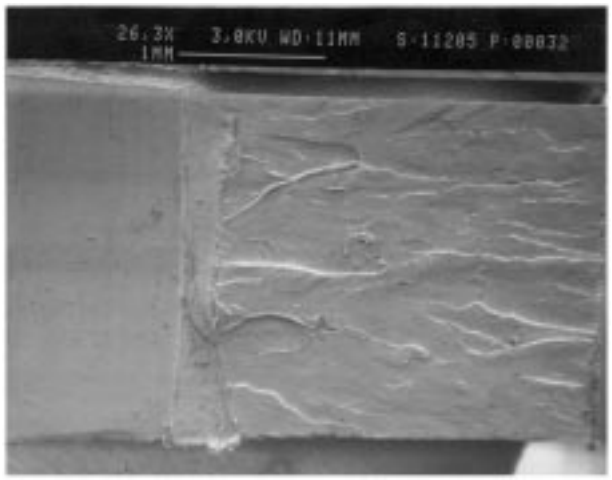

Figure 14 Uniaxial SRC-PMMA processed for 70 min at 128 °C. Fracture toughness is 2.82 ± 0.17 MPa m$^{1/2}$. Note the rippled appearance of the fracture surface. The crack propagates from left to right.

moderate temperatures, a mixed mode of fracture is seen, with the predominant mechanisms of matrix cracking and fiber cleavage or shearing occurring. The crack proceeds in a step-like fashion, fracturing fibers when the stress level has reached a critical level. Fiber splitting is also seen in some instances, but does not appear to contribute as significantly to the fracture as the other two mechanisms.

Long times and low temperatures or low times and high temperatures lead to a rippled fracture surface. This surface does not have the same fractographic characteristics as bulk acrylic, but it cannot be considered a fibrous material, either. The high temperature peaks found in DSC plots indicate that there is some retained molecular orientation, which apparently results in some strengthening.

5. Discussion

The goal of this work was to examine the effects of a range of processing conditions on fracture morphology,

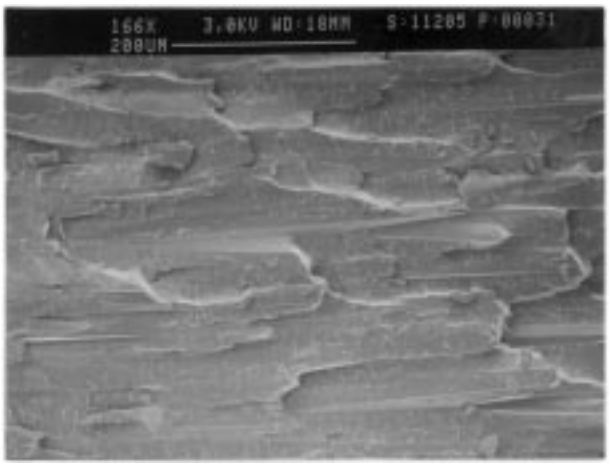

Figure 13 Appearance of exposed fracture surface of uniaxial SRC-PMMA processed for 58 min at 128 °C. Fracture toughness is 3.10 ± 0.26 MPa m$^{1/2}$. The fibers have lost their distinctive appearance and the fracture proceeds in a step-wise fashion, using a combination of matrix cracking and fiber shearing mechanisms.

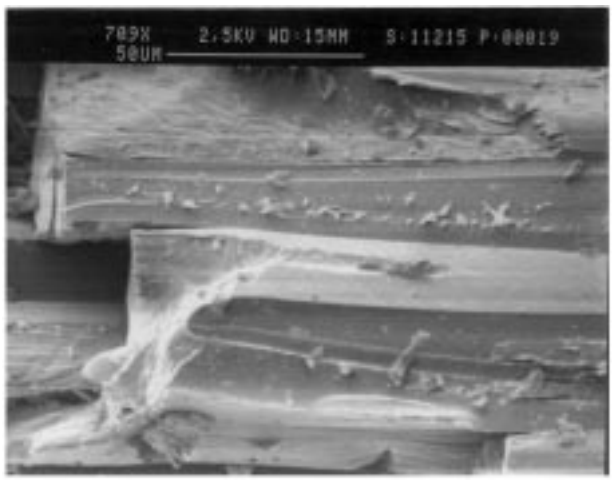

Figure 15 Fracture surface of uniaxial SRC-PMMA processed for 35 min at 140 °C. Fracture toughness is 2.36 ± 0.23 MPa m$^{1/2}$. Note that the fibers appear distinct. Matrix cracking and fiber cleavage can be seen. The crack propagates from right to left.

fracture toughness and thermal properties of a self-reinforced composite made from PMMA fibers with a high amount of molecular orientation. DSC tests showed that there are distinct endothermic and exothermic peaks which appear. There are two exothermic peak locations, located at temperature ranges of 130–135 °C and 145–160 °C. Exothermic peaks can be related to relaxation which occurs as the fibers lose the orientation imparted to them during processing. On a molecular level, the extended chain conformation in the oriented polymer is relaxing from a low entropy state (extended chains) to a high entropy state (random orientation). Endothermic peaks are related to the glass transition temperature at low temperatures, and may relate to other relaxation events such as main chain disentanglement and chain conformational changes at higher temperatures.

The exothermic peaks and the higher temperature endothermic peaks tend to diminish in magnitude or disappear altogether when processed at times greater than 65 min or at temperatures equal to 151 °C. These samples generally exhibited more brittle fracture. Thus, the presence or absence of specific peaks may predict the mechanical properties of the composite.

SEM analysis shows five distinct fracture mechanisms. The first is matrix cracking (i.e. interfiber fracture), which occurs in composites with weak interfacial bonding between fibers. Composites with weak interfaces have the lowest fracture toughnesses. The second is fiber cleavage, which occurs in conjunction with matrix cracking in composites with moderate to high fracture toughnesses. The third is fiber splitting, which occurs to a small degree in all of the composites which still have distinct fibers present in the composite. The fourth mechanism is brittle fracture, which occurs in bulk PMMA, and the fifth mechanism is a rippled fracture surface which occurs in composites which have lost most of the fiber's molecular orientation.

5.1. DSC tests

The heating rate chosen for these DSC experiments, $80\,^{\circ}C\,min^{-1}$ is significantly higher than the usual heating rates [23] used for polymer samples (5–$20\,^{\circ}C\,min^{-1}$). The increase in heating rate increases the temperatures at which transitions occur [23] and can also induce artefacts caused by the balance between thermal lag in the sample and equilibrium conditions [23]. In order to ensure that the effects seen in these results are not merely an artefact of the heating rate, SRC-PMMA samples processed for 40 min at 128 °C were tested at heating rates of 5, 10, 20, 40 and $80\,^{\circ}C\,min^{-1}$. At heating rates of $10\,^{\circ}C\,min^{-1}$ and higher, an increased heat capacity in the oriented material was seen both above and below T_g. The exothermic peak decreased in magnitude with decreasing heating rate, and was still visible at a heating rate of $20\,^{\circ}C\,min^{-1}$. As the heating rate decreased, the noise present in the signal increased substantially, leading to difficulty in identifying individual peaks. It is believed that a heating rate of $80\,^{\circ}C\,min^{-1}$ amplifies the non-equilibrium events that are occurring in the relaxation of the oriented polymers while minimizing the noise in the data acquisition system.

A unique part of these DSC tests was the testing of a single sample several times. This allowed for alignment of DSC scans before and after the molecular orientation had been lost, and a repeatable baseline for comparison. Since the second, third and fourth scans were all perfectly superimposed on one another with this method, the exothermic and endothermic peaks seen in the first scan of the oriented material are not artefacts, but representative of relaxation events that are occurring and changes in the structure of the oriented polymer.

5.2. Optimal processing of SRC-PMMA

One limitation of these results is the unknown pressure placed on these samples during processing. Pressure has been assumed to be constant throughout processing, and between samples. The c-clamps often provided uneven pressure, leading to samples which were not rectangular in cross-section, but trapezoidal. This effect can be seen as color variations when the samples are viewed in polarized light. In addition, when the samples are removed from the oven after processing, the sample has consolidated so much that the clamps are loose and need to be retightened. Pressure, therefore, is unknown and not constant during the processing period. This study utilized enough pressure to consolidate fibers into polygonal space-filling shapes and allow sintering between fibers to take place. At this time, it is unknown what effect changing pressure has on the properties of SRC-PMMA. Therefore, even though the samples were sectioned from adjacent locations, and the edges of the bar were unused, these pressure differences may lead to different physical properties and variation between samples.

The fracture mechanisms and DSC results lead to the discussion of competing mechanisms occurring in the processing of these composite materials. Two mechanisms are competing: fiber–fiber bonding (incorporation) and loss of retained molecular orientation. The consolidation of these materials occurs as the outer polymer of adjacent fibers soften and interdiffuse. When this process is not completed, it results in a weak interface and interfacial cracking, as shown in the low time and temperature samples. However, when processing continues for too long a time or at too high a temperature, most of the molecular orientation in the fibers is lost. The matrix has reached a theoretical maximum bonding strength, but the majority of the strengthening gained from the molecular orientation of the fibers has been lost.

Thus, there would then be an optimal location where both of these quantities are at a maximum. This concept is schematically shown in Fig. 16. From the fracture toughness results, it appears that an optimum sample can be processed at 128 °C for 65 min. This sample yields a fracture toughness of $3.18 \pm 0.30\,MPa\,m^{1/2}$, and has a flat fracture surface in three out of the four samples tested. The bulk of the fracture surface is similar to the rippled surface shown in Fig. 14. At the crack tip, however, fibers are outlined by matrix cracking (interfiber fracture) in a manner similar to that depicted in Fig. 12. The sample processed for 65 min at 128 °C optimizes the strength at the matrix and the retained molecular orientation of the fibers to maximize the

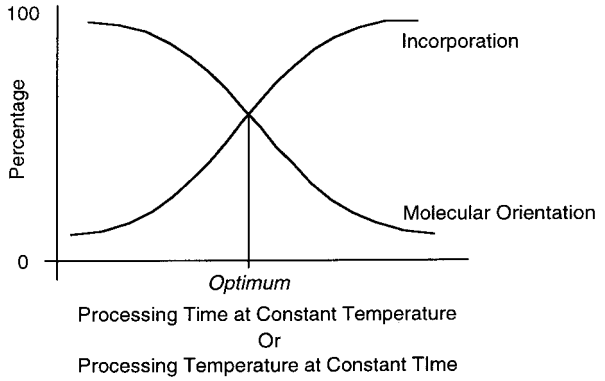

Figure 16 Hypothetical relationship between retained molecular orientation and incorporation of the composite material. Theoretically, the maximum composite properties would be realized at the optimum point between these two quantities.

fracture toughness of the composite. DSC results yielded a small exothermic peak in the 150–175 °C range in two out of the three samples tested, and endothermic peaks at the same locations as the other samples tested. The exothermic peak indicates that there is some retained molecular orientation in the fibers. This is not the only optimum sample, however. Theoretically, different temperatures may produce other optimum samples, such as those shown in Fig. 8, fracture toughness increases with increasing processing temperature at a constant time.

Theoretically, there is an optimum balance between molecular orientation and incorporation which will lead to the highest mechanical property, as shown in Fig. 16. This idea can be extended to a three-dimensional surface where it can be hypothesized that a mechanical property can be plotted versus time and temperature to form a surface with a ridge of optimal mechanical properties. This ridge would represent a set of processing conditions which would lead to a maximum in the mechanical property being measured. In addition, the set of processing conditions for optimal fracture toughness may not be the same as the optimal processing condition for another mechanical property, such as fatigue. One could imagine in Fig. 16 that each mechanical property requires a unique molecular orientation and bond strength between fibers to attain the optimal mechanical property. Furthermore, the time and temperature may also be sensitive to the actual processing method, molds used, and pressure generating devices. Similarly, rates of heating and cooling, pressure cycles and other factors may influence the time and temperature needed to make optimum composites and may raise (or lower) the relative location of the optimum mechanical property as depicted schematically in Fig. 16.

5.3. Relating thermal and mechanical properties

To link thermal and mechanical properties, comparisons should be made between samples which have been processed in different ways and produce strengths and thermal characteristics which are similar. In this way, a DSC fingerprint may then predict a mechanical strength independent of the processing conditions. For example, comparing samples processed for 70 min at 128 °C and for 35 min at 151 °C, these samples have statistically the same fracture toughness. DSC results are also seen to be similar when Figs 2 and 3 are compared. The general shape and location of the peaks is very similar. Also note that these DSC scans bear less resemblance to the other DSC figures than to each other. Finally, the fracture morphologies of these samples are very similar. They both exhibit rippled fracture surfaces, as seen representatively in Fig. 14. Based on this representative comparison, it can be seen that thermal and mechanical properties can be linked to one another.

6. Conclusions

DSC analysis showed that SRC-PMMA has unique and measurable exothermic and endothermic events which change with length of processing time and temperature. These peaks are presumably related to molecular relaxation events which occur as the oriented composite material assumes a random configuration.

The mechanical fracture toughness properties of the composites also varies with processing parameters, reaching a maximum of $3.18 \pm 0.30\,\mathrm{MPa\,m^{1/2}}$ at a temperature of 128 °C, and processing time of 65 min. For constant time processing of 35 min, the fracture toughness increases in the temperature range of 128–151 °C, but does not reach a maximum. Changes in the fracture toughness can be related to the five mechanisms found in microscopy of fracture surfaces: matrix cracking, fiber cleavage, fiber splitting, brittle fracture, and rippled fracture.

DSC and fracture toughness are shown to be methods which can evaluate the thermal and mechanical properties of SRC-PMMA. These methods can then be used to investigate the effects of processing on the properties of these composite materials.

Although an absolute optimum processing parameter has not been defined, it has been shown that processing has an effect on the consolidation of the composite, retained molecular orientation of the fibers, the resultant mechanical properties and the fracture mechanisms.

Acknowledgment

The authors would like to acknowledge Atohaas for the donation of PMMA and Zimmer Inc. for their assistance in the fiber spinning portion of this work. This material is based upon work supported under a National Science Foundation Graduate Research Fellowship.

References

1. W. J. MALONEY, M. JASTY, D. W. BURKE, D. O. O'CONNER, E. B. ZALENSKI, C. BRAGDON and W. H. HARRIS, *Clin. Orthop. Rel. Res.* **249** (1989) 129.
2. L. D. T. TOPOLESKI, P. DUCHEYNE and J. M. CUCKLER, *J. Biomater. Res.* **24** (1990) 135.
3. S. P. JAMES, M. JASTY, J. DAVIES, H. PIEHLER and W. H. HARRIS, *ibid.* **26** (1992) 651.
4. S. SAHA and S. PAL, *ibid.* **20** (1986) 817.
5. K. EKSTRAND, I. E. RUYTER and H. WELLENDORF, *ibid.* **21** (1987) 1065.

6. B. POURDEYHIMI, H. H. ROBINSON IV, P. SCHWARTZ and H. D. WAGNER, *Ann. Biomed. Engng* **14** (1986) 277.
7. C. A. BUCKLEY, E. P. LAUTENSCHLAGER and J. L. GILBERT, *J. Appl. Polym. Sci.* **44** (1992) 1321.
8. J. L. GILBERT, D. S. NEY and E. P. LAUTENSCHLAGER, *Biomaterials* **16** (1995) 1043.
9. D. D. WRIGHT, E. P. LAUTENSCHLAGER and J. L. GILBERT, *J. Biomater. Res.* **36** (1997) 441.
10. P. TÖRMÄLÄ, J. VASENIUS, S. VAINIONPÄÄ, J. LAIHO, T. POHJONEN and P. ROKKANEN, *ibid.* **25** (1991) 1.
11. S. FERGUSON, D. WAHL and S. GOGOLEWSKI, *ibid.* **30** (1996) 543.
12. M. I. ABO EL-MAATY, D. C. BASSETT, R. H. OLLEY, P. J. HINE and I. M. WARD, *J. Mater. Sci.* **31** (1996) 1157.
13. J. RASBURN, P. J. HINE, I. M. WARD, R. H. OLLEY, D. C. BASSETT and M. A. KABEEL, *ibid.* **30** (1995) 615.
14. P. J. HINE, I. M. WARD, R. H. OLLEY and D. C. BASSETT, *ibid.* **28** (1993) 316.
15. M. A. KABEEL, D. C. BASSETT, R. H. OLLEY, P. J. HINE and I. M. WARD, *ibid.* **29** (1994) 4694.
16. *Idem.*, *ibid.* **30** (1995) 601.
17. R. H. OLLEY, D. C. BASSETT, P. J. HINE and I. M. WARD, *ibid.* **28** (1993) 1107.
18. B. TISSINGTON, G. POLLARD and I. M. WARD, *ibid.* **26** (1991) 82.
19. ASTM Specification E399. In ASTM Standards, Philadelphia, PA, USA: ASTM, 1985.
20. F. RODRIGUEZ, ''Principles of polymer systems,'' (Hemisphere Publishing Corporation, New York, 1982).
21. B. WUNDERLICH, ''Thermal analysis,'' (Academic Press, Inc., Boston, 1990).
22. J. F. KNOTT, ''Fundamentals of fracture toughness,'' (Butterworths, London, 1973).
23. I. W. GILMOUR and J. N. HAY, *Polymer* **18** (1977) 281.

Received 28 January
and accepted 19 August 1998